Electronic Supplementary Information

Iron amino-bis(phenolate) complexes for the formation of organic carbonates from CO_2 and oxiranes

Dalal Alhashmialameer,[a] Julie Collins,[b] Karen Hattenhauer,[a] and Francesca M. Kerton*[a]

[a] Department of Chemistry, Memorial University of Newfoundland, St. John's, Newfoundland, Canada A1B 3X7. E-mail: fkerton@mun.ca; Tel:

[b] C-CART X-ray Diffraction Laboratory, Memorial University of Newfoundland, St. John's, Newfoundland.

Table S1. Crystallographic data and structure refinement for **1**and **2**.

Compound	**1**	**2**
Empirical Formula	$C_{35}H_{54}FeClN_2O_3.C_3H_6O$	$C_{29}H_{42}FeClN_2O_2{\cdot}0.5C_3H_6O_1$
CCDC no.	1452392	1452393
Formula Weight	684.18	570.98
Temperature/K	138	168
Crystal Color	Purple	Purple
Crystal System	Monoclinic	Monoclinic
Crystal Dimensions	0.3 X 0.3 X 0.17 mm	0.29 × 0.2 × 0.2 mm
Lattice Parameters	a = 12.492(3) Å	a = 27.898(9) Å
	b = 9.7027(19) Å	b = 9.683(3) Å
	c = 31.799(6) Å	c = 23.472(8) Å
	α = 90°	α = 90°
	β = 94.843(3)°	β = 110.032(4)°
	V = 3840.6(13) Å^3	V = 5957(3) Å
Space Group	$P2_1/n$	C2/c
Z value	4	8
D_{calc}	1.183 g/mm^3	1.273 g/cm^3
F_{000}	1476.0	2440.0
μ(MoKα)	0.498 mm^{-1}	0.627 cm^{-1}
Reflections collected	34918	27235
Independent reflections	8486	6525
R_{int}	0.0417	0.0380
R, wR_2 (all)[a]	0.0417, 0.1025	0.0392, 0.1006
R, wR_2 [I>=2σ (I)][a]	0.0400, 0.1039	0.0375, 0.0988
GOF-fit on F^2	1.051	1.051

$$^{a}R_1 = \Sigma(|F_o| - |F_c|)/\Sigma|F_o| \; ; \; wR_2 = [\, \Sigma(w(F_o^2 - F_c^2)^2)/\ \Sigma w(F_o^2)^2]^{1/2}$$

Table S2. Selected Bond lengths (Å) and angles (°) for **1** and **2**.

	1	**2**
Fe-O(1)	1.8696(12)	1.8805(12)
Fe-O(2)	1.8734(11)	1.8690(12)
Fe-N(1)	2.1864(13)	2.1826(14)
Fe-N(2)	2.1681(13)	2.1902(14)
Fe-Cl	2.2466(6)	2.2488(8)
O(1)-Fe-O(2)	97.34(5)	98.85(5)
O(1)-Fe-Cl	111.90(4)	109.07(4)
O(2)-Fe-Cl	110.54(4)	110.41(4)
N(1)-Fe-Cl	97.84(4)	99.25(4)
N(2)-Fe-Cl	98.54(4)	96.29(4)
O(1)-Fe- N(1)	86.06(5)	87.84(5)
O(1)-Fe- N(2)	145.15(5)	145.20(5)
O(2)-Fe- N(2)	87.01(5)	86.22(5)
O(2)-Fe- N(1)	147.45(5)	150.19(5)
N(1)-Fe- N(2)	72.93(5)	72.46(5)

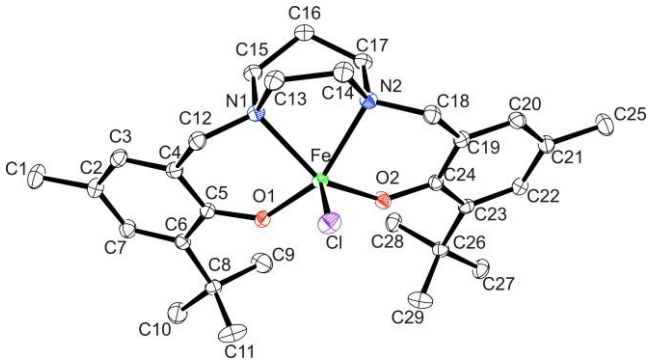

Figure S1. Molecular structure (ORTEP) and partial numbering scheme for **2**. Ellipsoids are shown at the 50% probability level (H-atoms omitted for clarity).

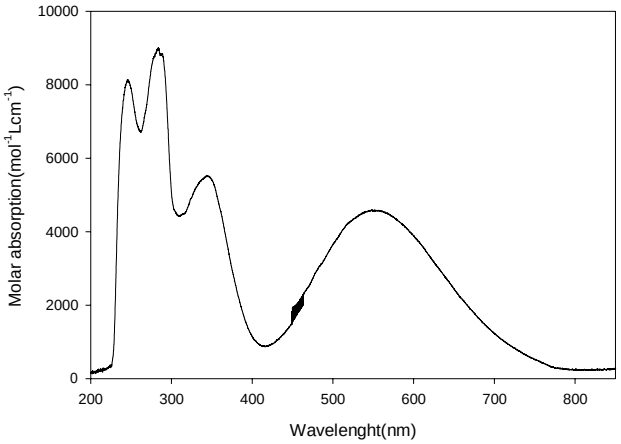

Figure S2. Electronic absorption spectrum of **2** in dichloromethane.

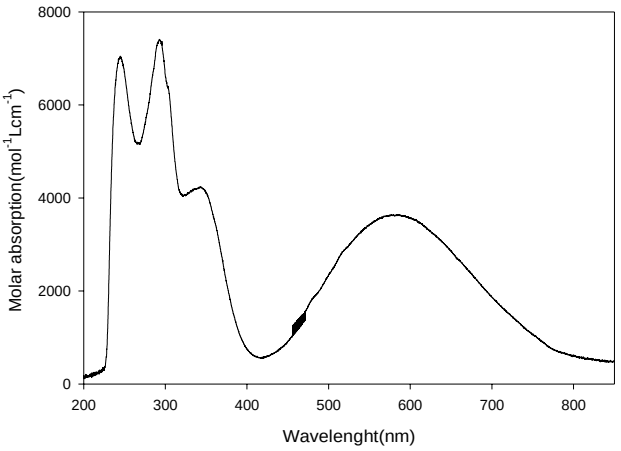

Figure S3. Electronic absorption spectrum of **3** in dichloromethane.

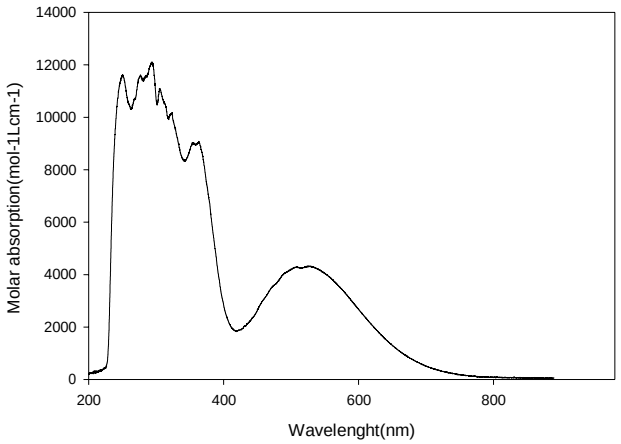

Figure S4. Electronic absorption spectrum of **4** in dichloromethane.

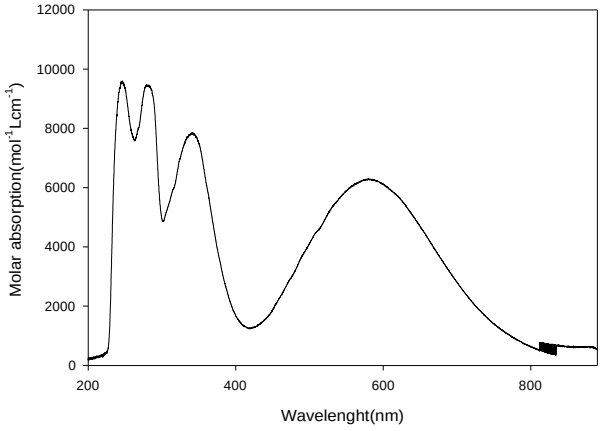

Figure S5. Electronic absorption spectrum of **5** in dichloromethane.

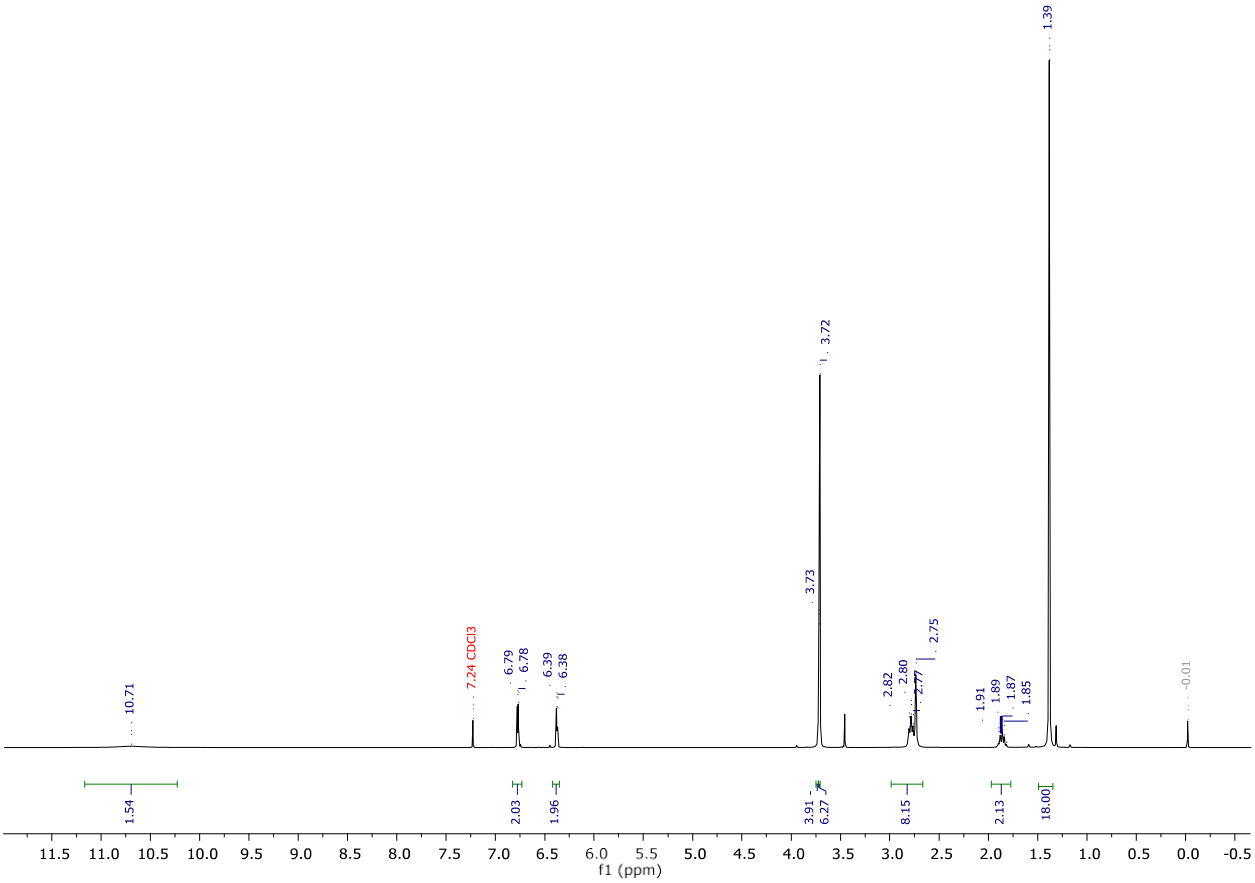

Figure S6. ^{1}H NMR spectrum (300 MHz, 298 K, $CDCl_3$) of **H_2L3**.

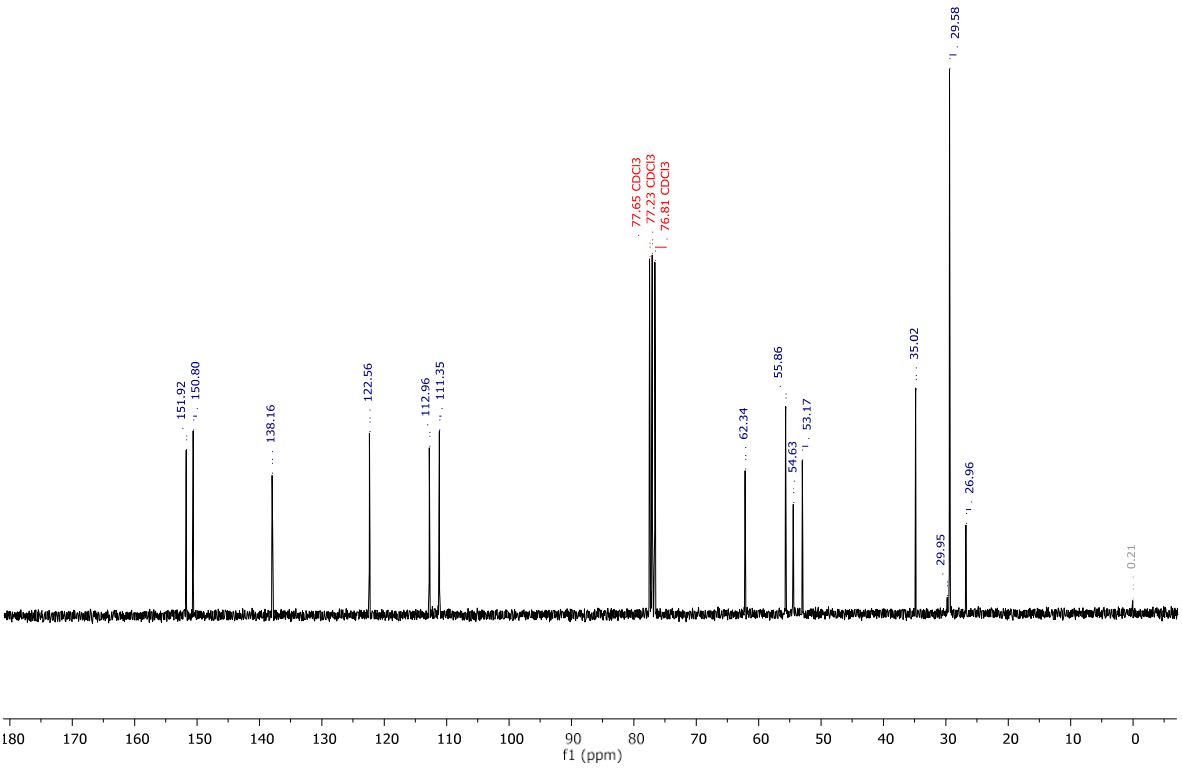

Figure S7. ^{13}C NMR spectrum (300 MHz, 298 K, $CDCl_3$) of **H_2L3**.

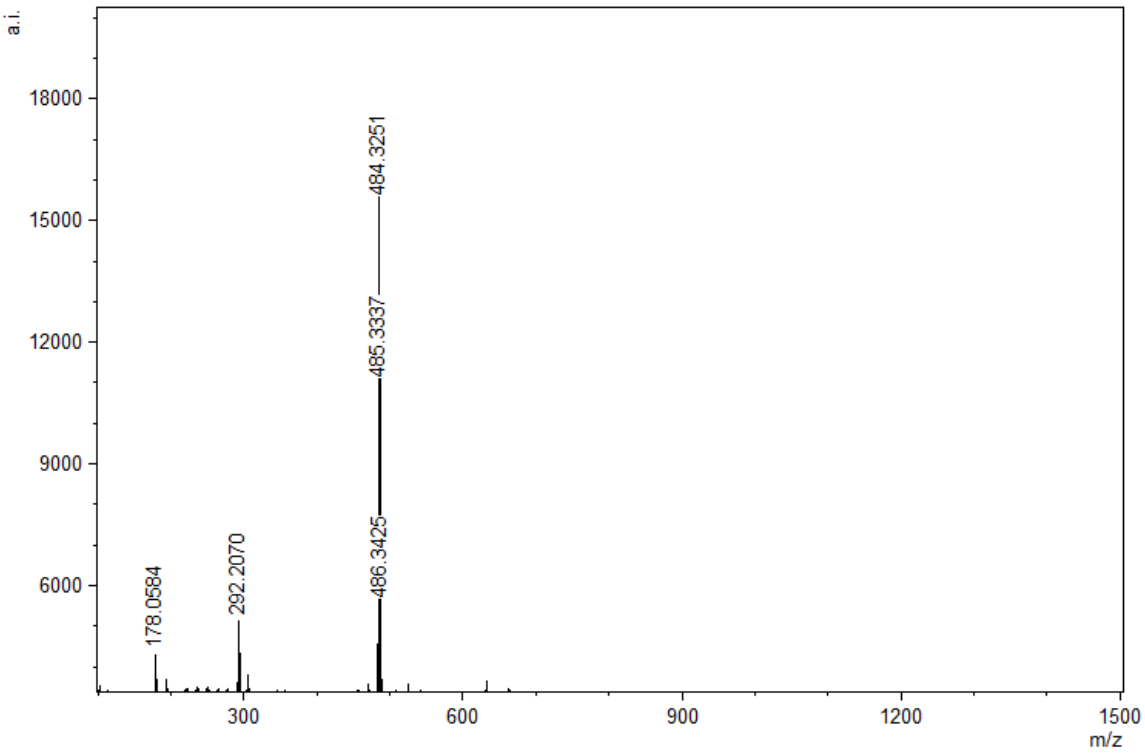

Figure S8. MALDI-TOF mass spectrum of **H_2L3**.

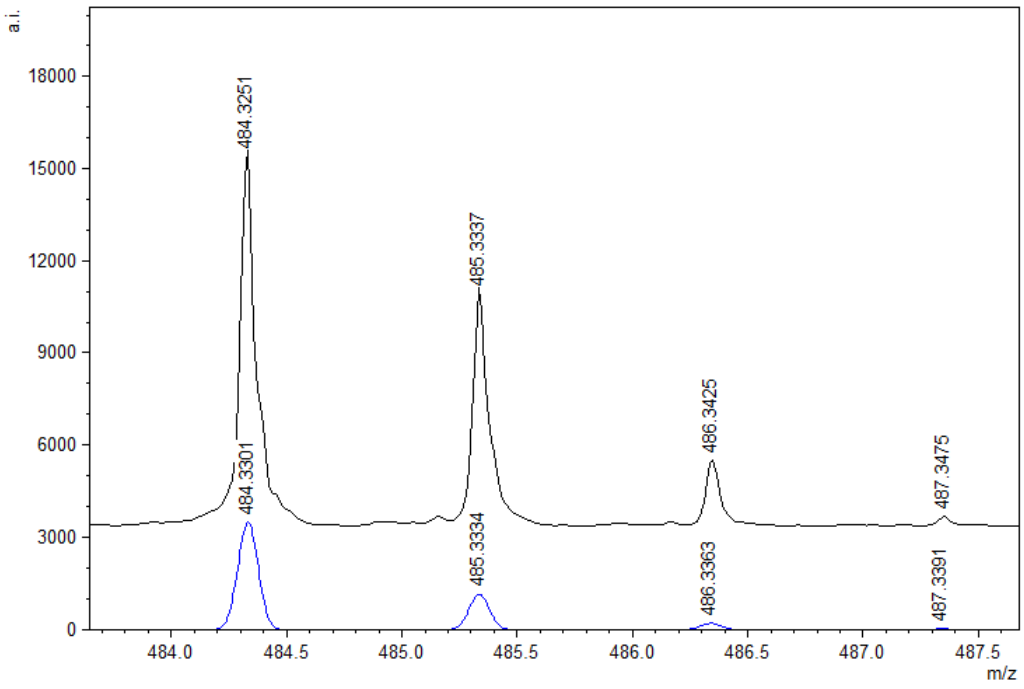

Figure S9. Theoretical and Experimental isotopic distribution pattern for **H_2L3**.

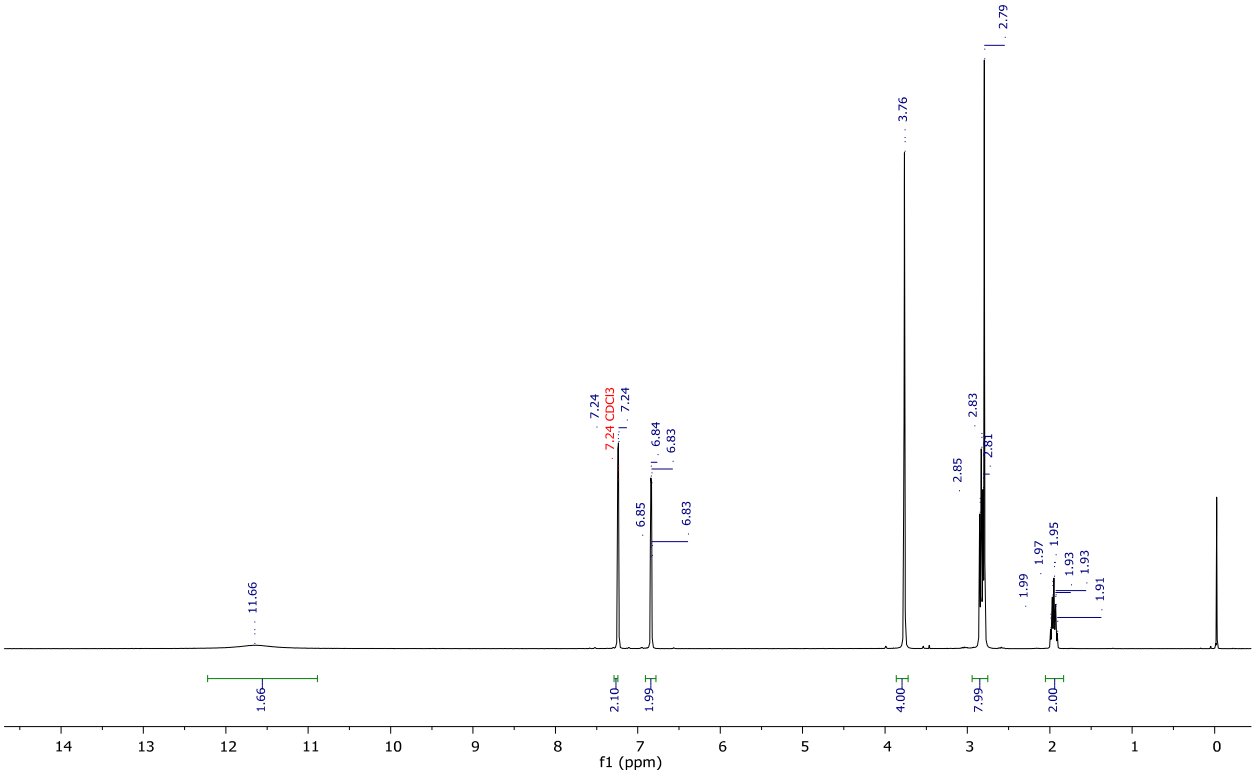

Figure S10. ^{1}H NMR spectrum (300 MHz, 298 K, $CDCl_3$) of **H_2L4**.

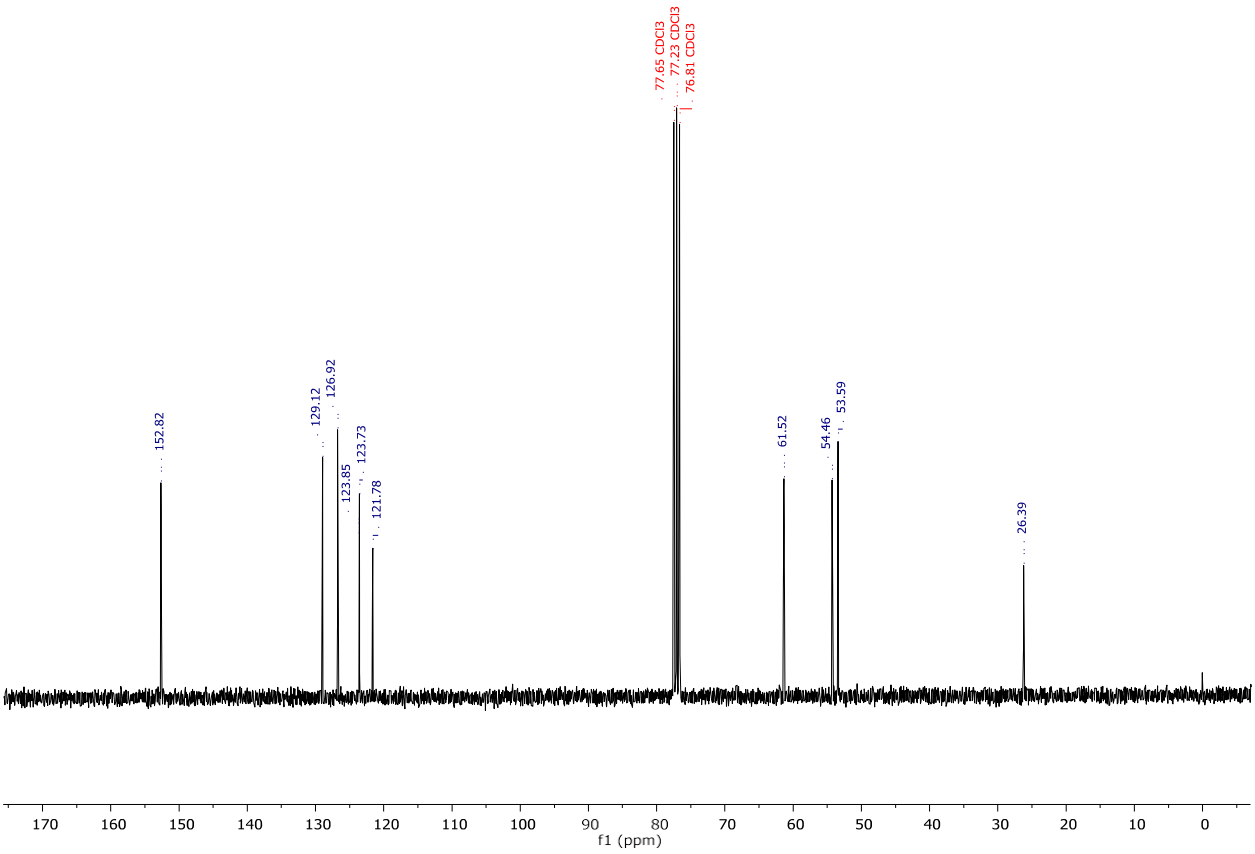

Figure S11. ^{13}C NMR spectrum (300 MHz, 298 K, $CDCl_3$) of **H_2L4**.

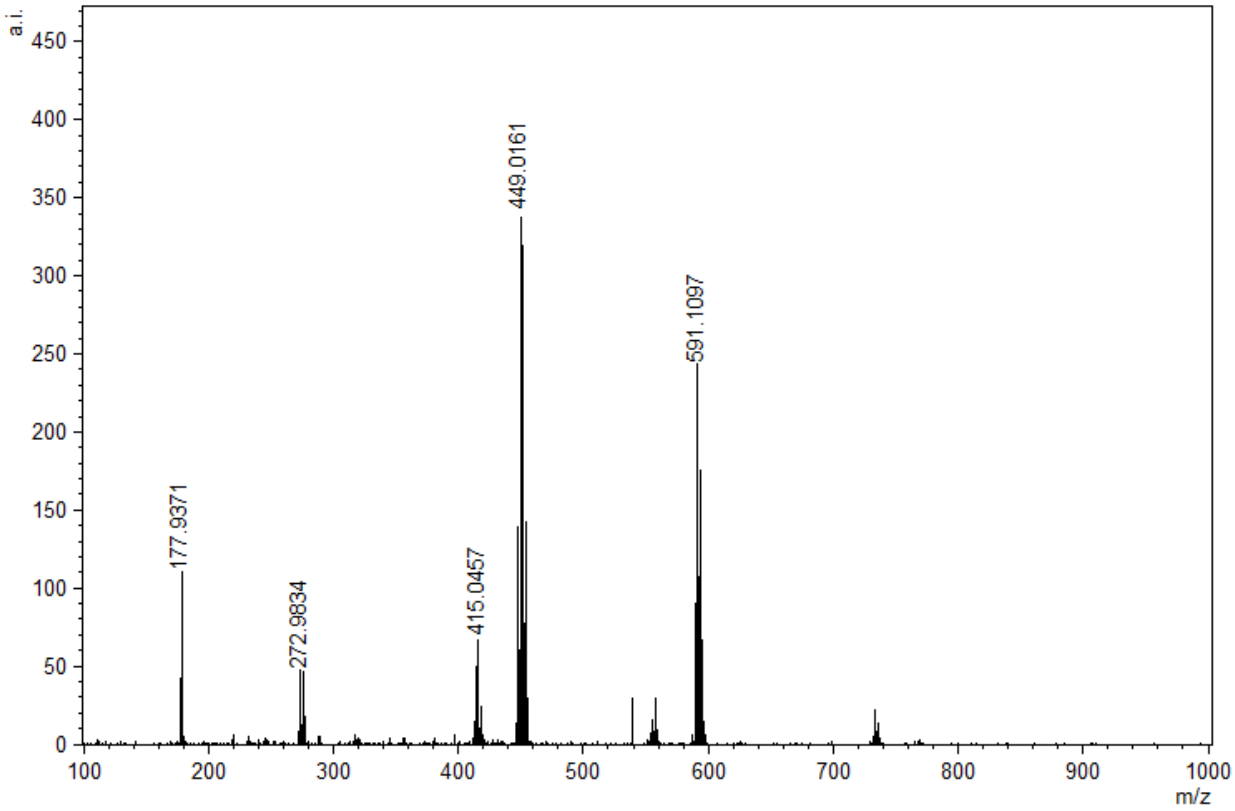

Figure S12. MALDI-TOF mass spectrum of **H_2L4**.

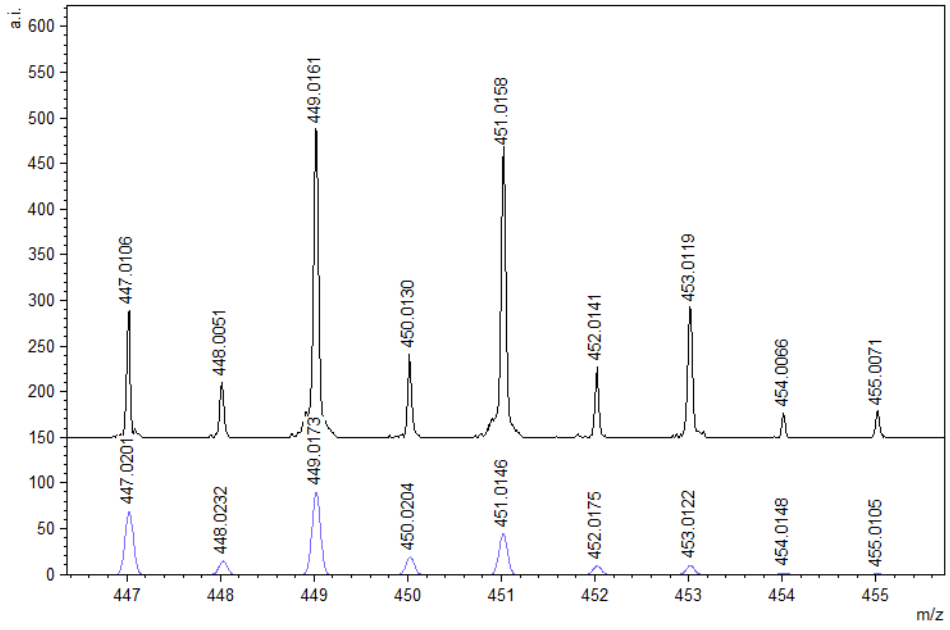

Figure S13. Theoretical and Experimental isotopic distribution pattern for **H_2L4**.

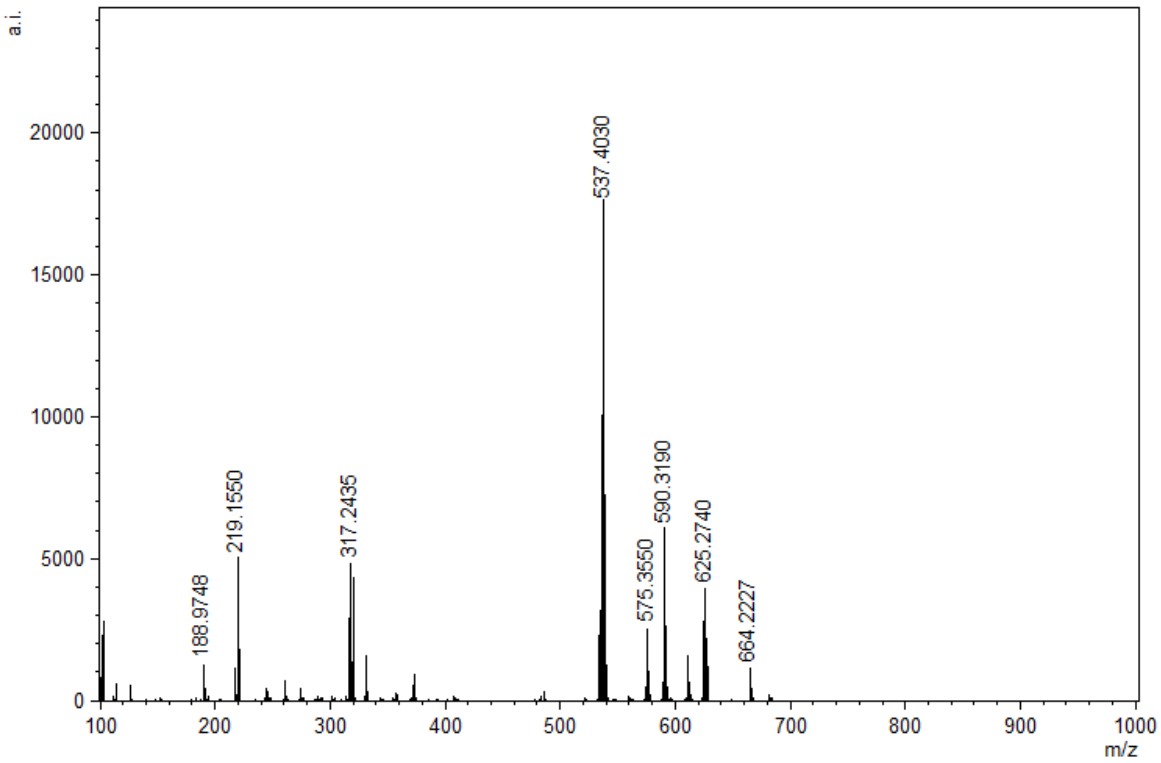

Figure S14. MALDI-TOF mass spectrum of **1**.

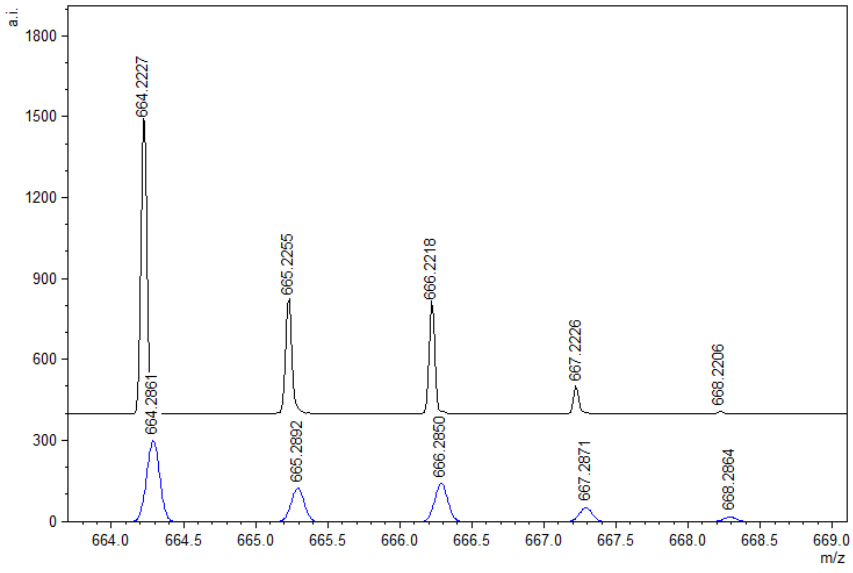

Figure S15. Theoretical and Experimental isotopic distribution pattern for **1** with K.

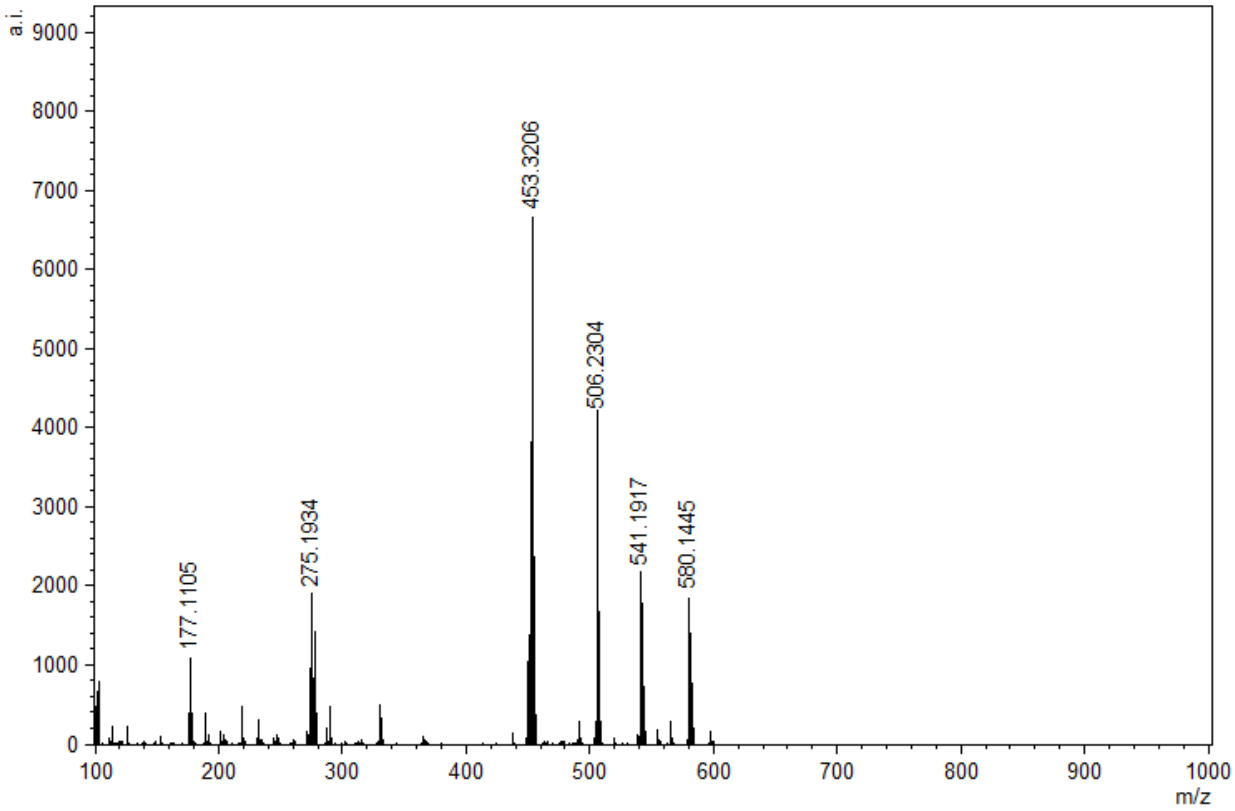

Figure S16. MALDI-TOF mass spectrum of **2**.

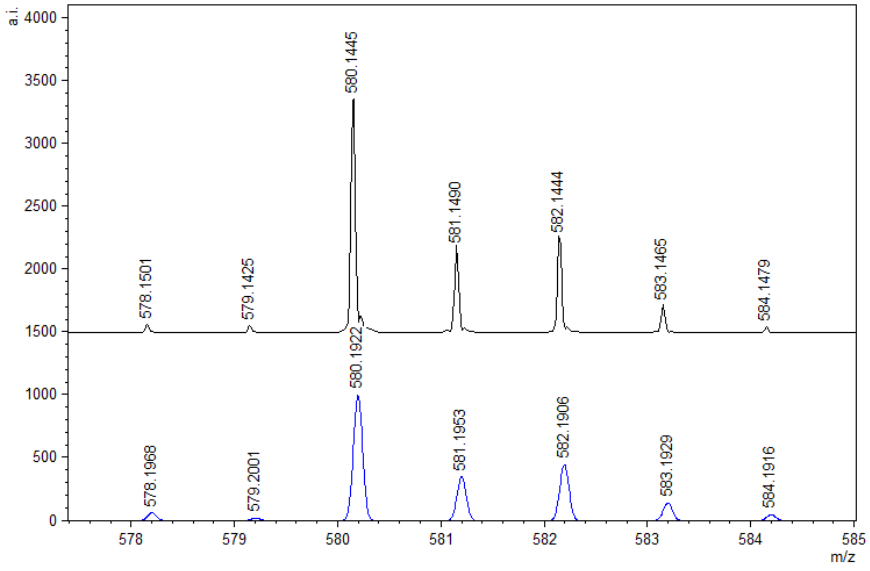

Figure S17. Theoretical and Experimental isotopic distribution pattern for **2** with K.

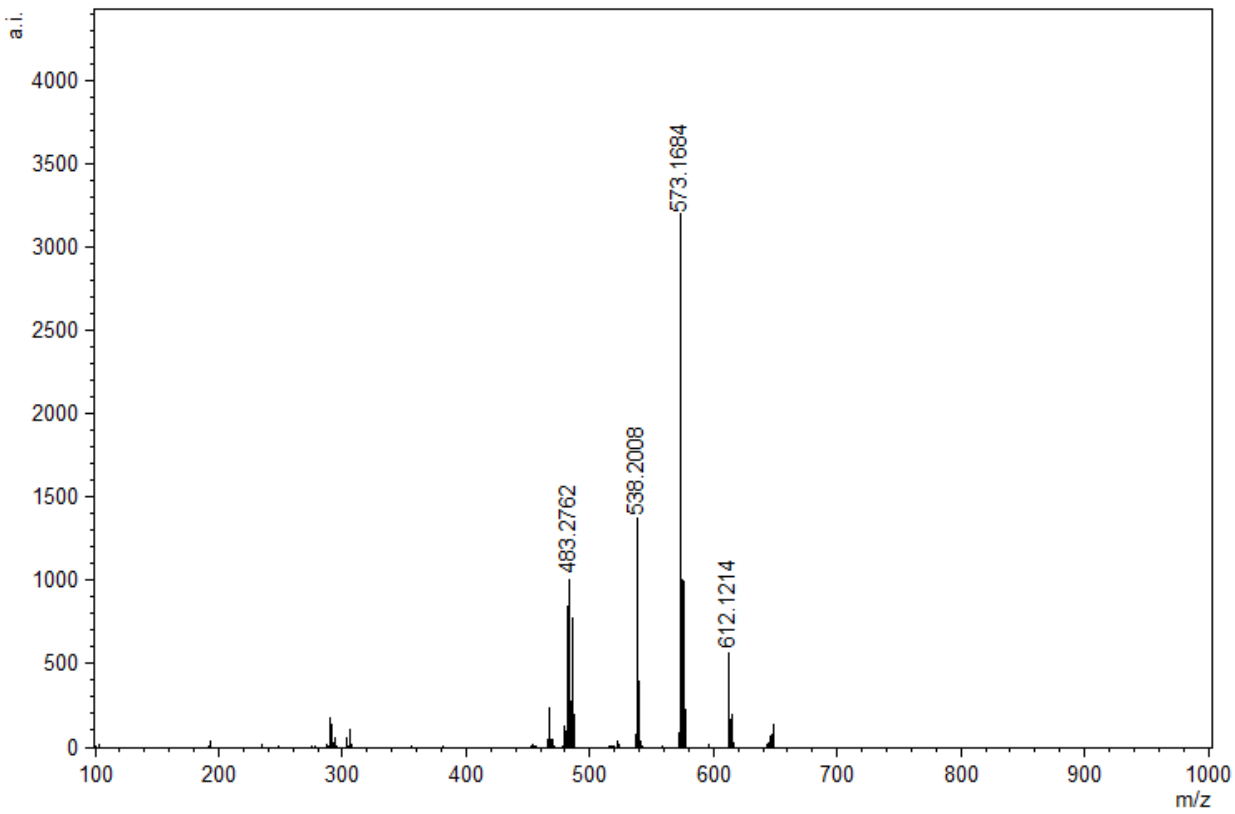

Figure S18. MALDI-TOF mass spectrum of **3**.

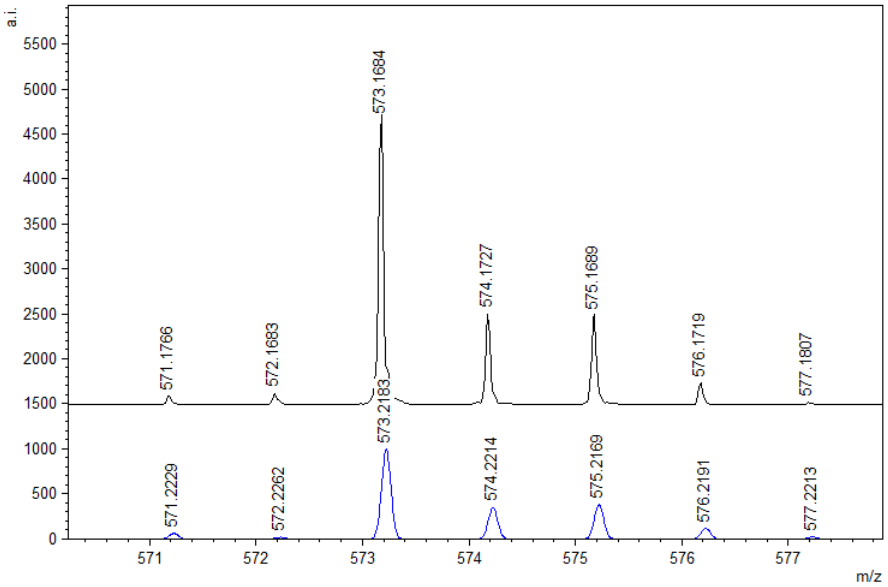

Figure S19. Theoretical and Experimental isotopic distribution pattern for **3**.

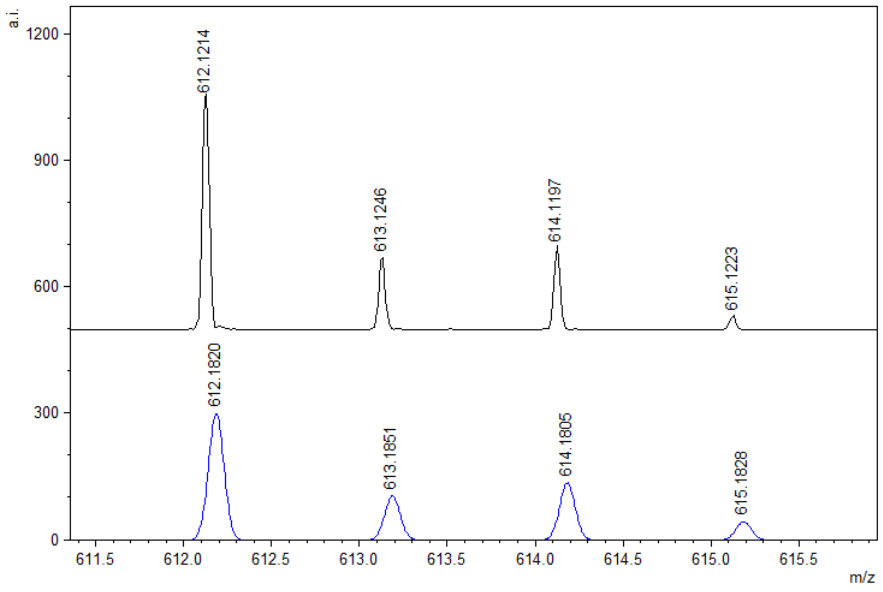

Figure S20. Theoretical and Experimental isotopic distribution pattern for **3** with K.

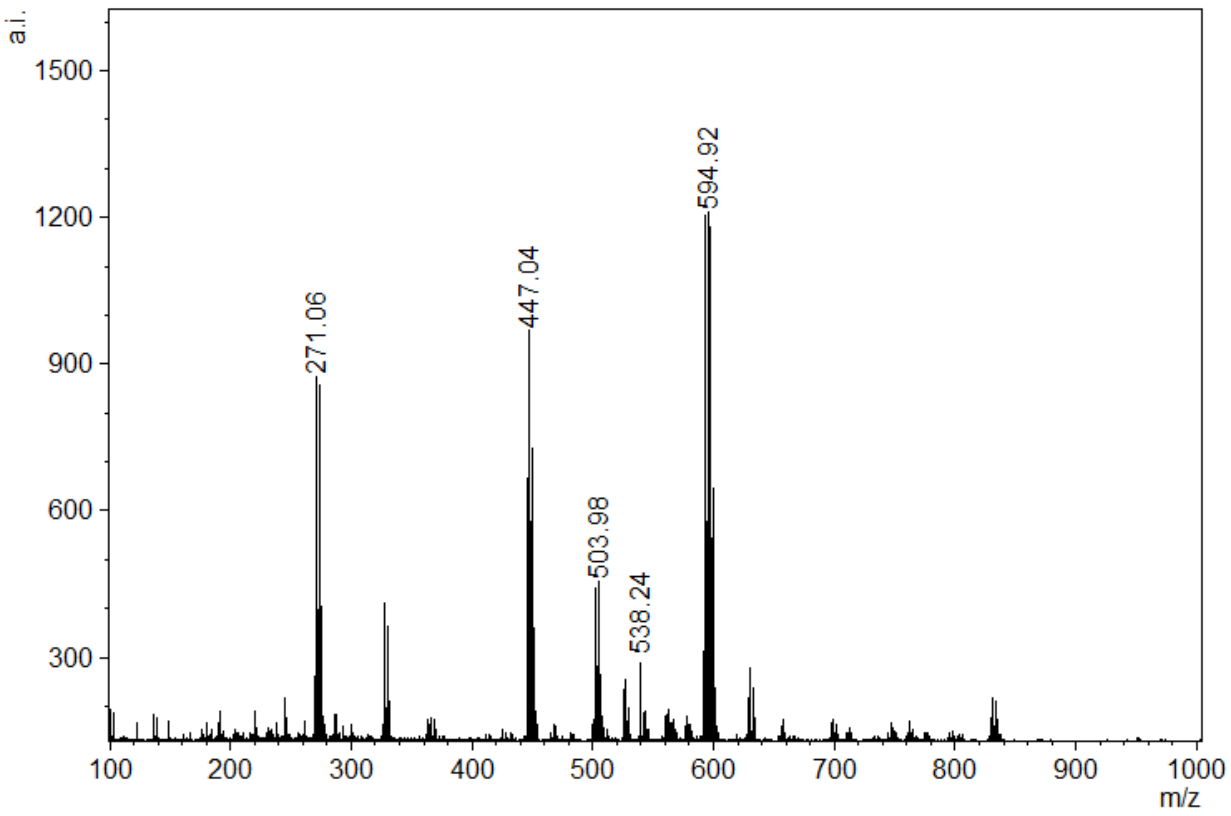

Figure S21. MALDI-TOF mass spectrum of **4**.

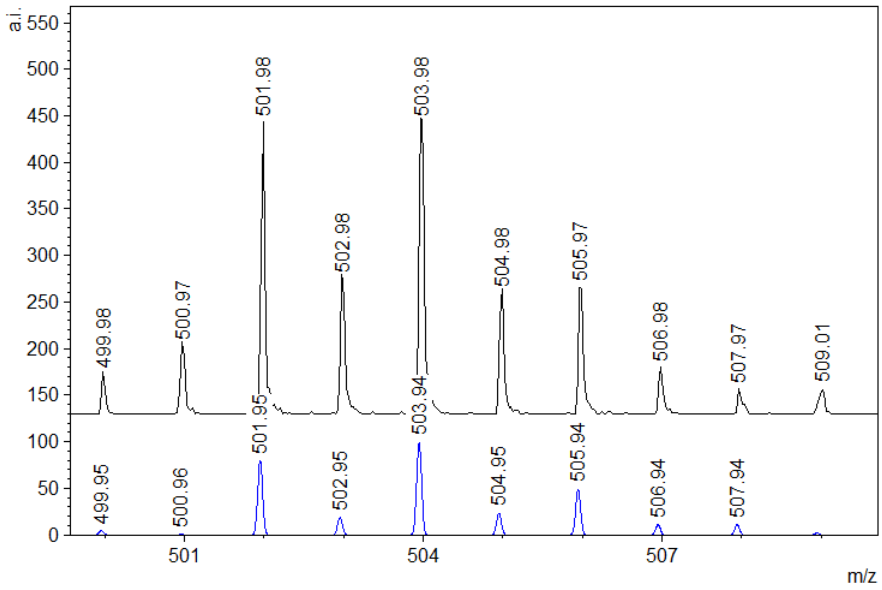

Figure S22. Theoretical and Experimental isotopic distribution pattern for **4**.

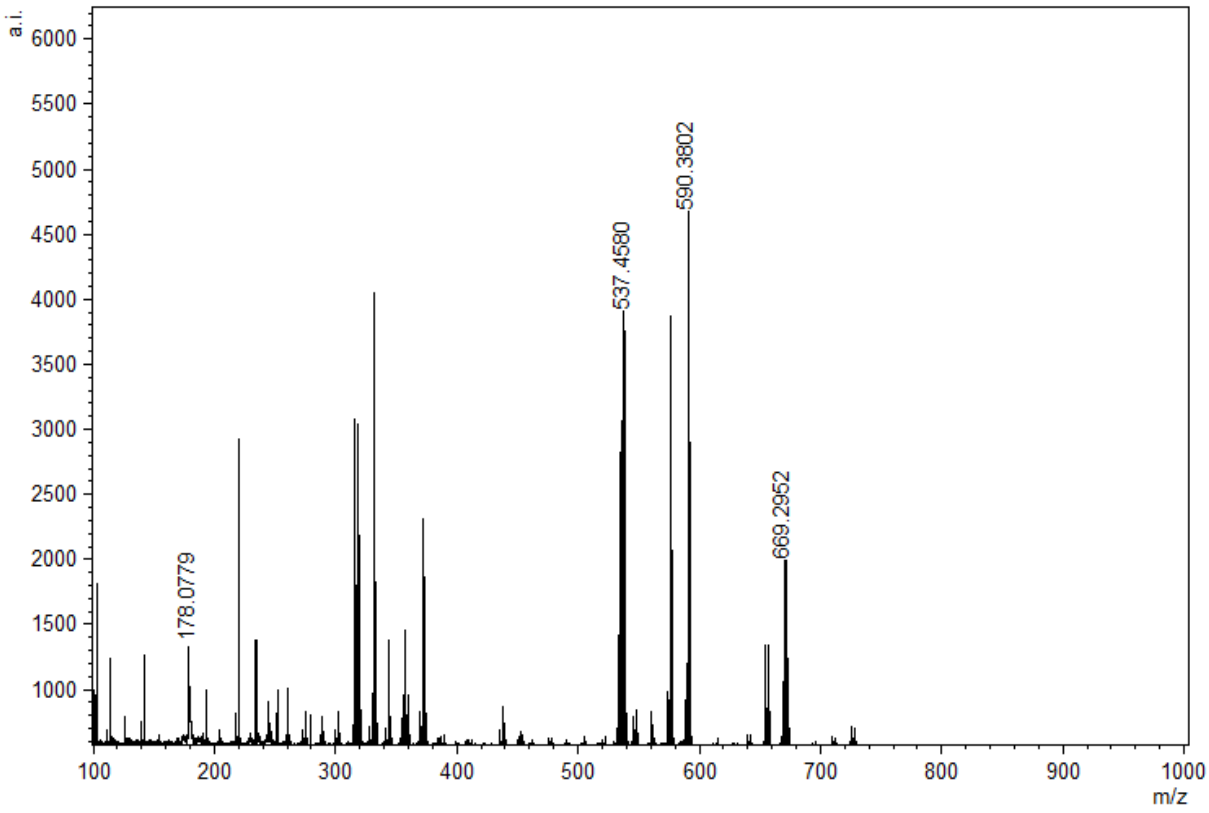

Figure S23. MALDI-TOF mass spectrum of **5**.

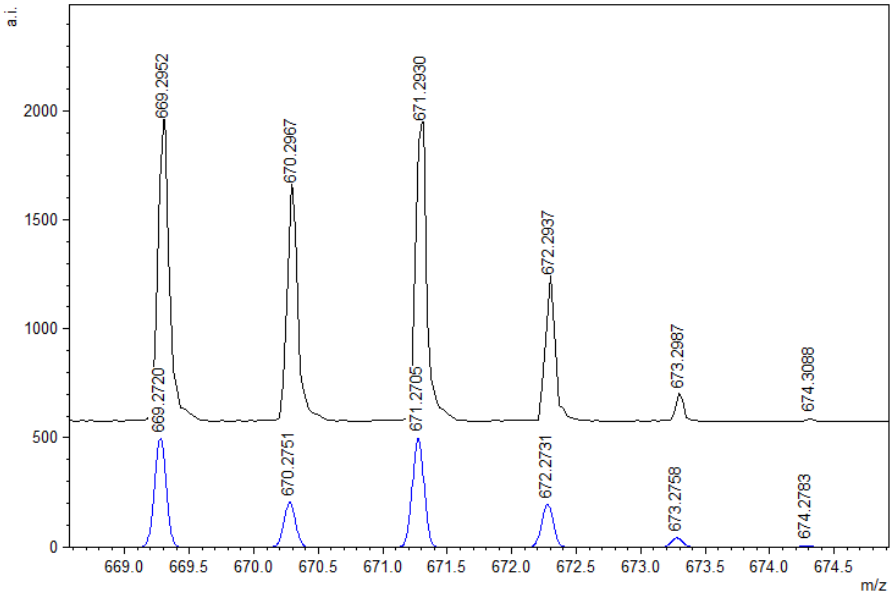

Figure S24. Theoretical and Experimental isotopic distribution pattern for **5**.

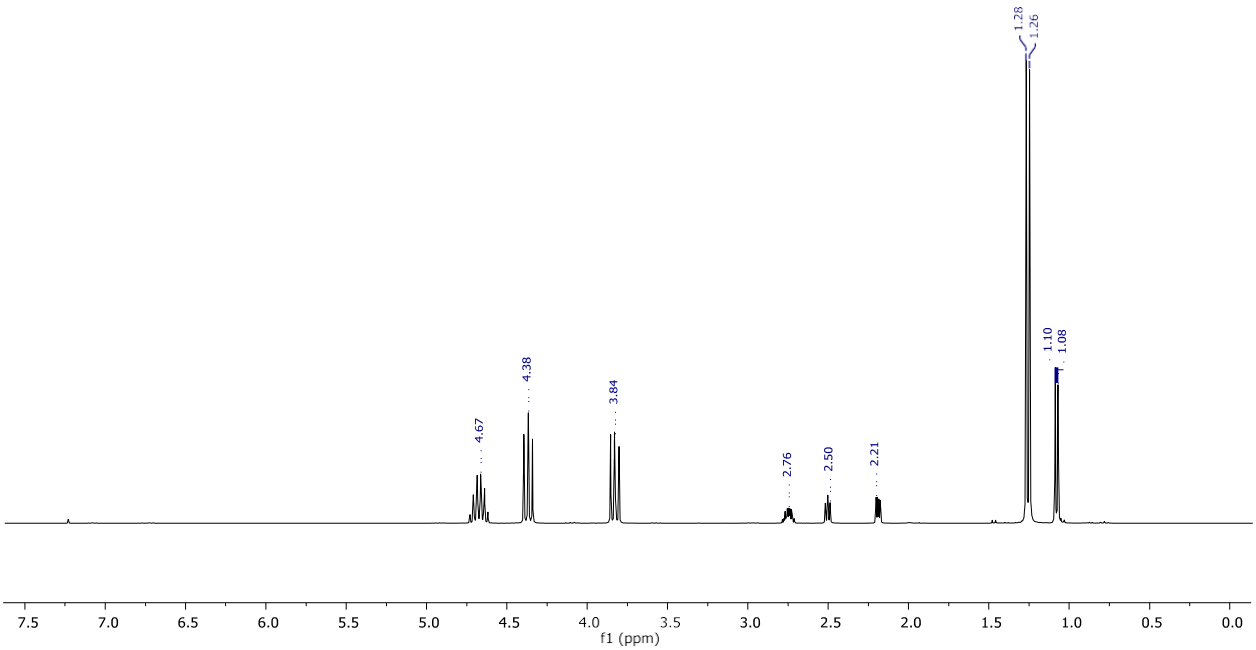

Figure S25. ^{1}H NMR spectrum (300 MHz, 298 K, $CDCl_3$) of 4-methyl-1,3-dioxolan-2-one (Table 2, entry 1).

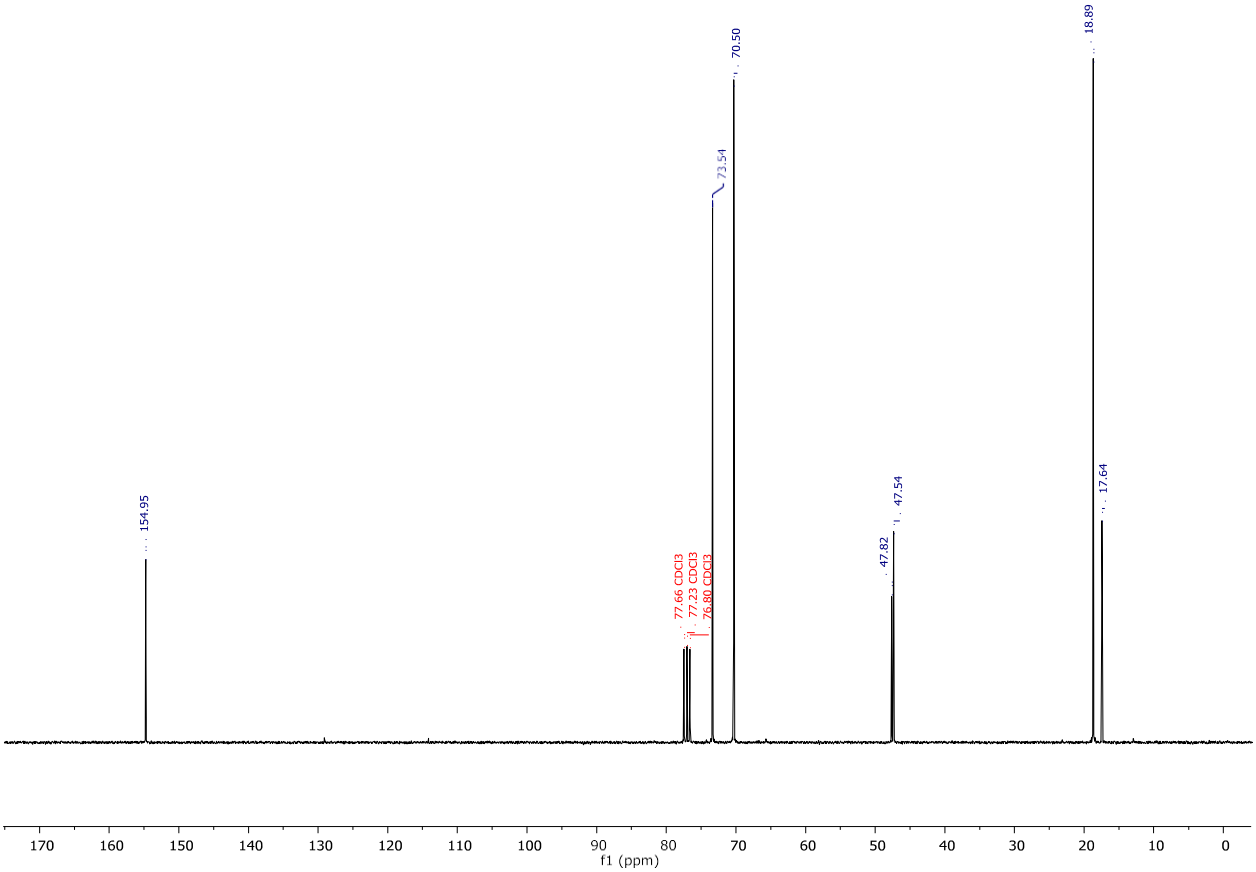

Figure S26. ^{13}C NMR spectrum (300 MHz, 298 K, $CDCl_3$) of 4-methyl-1,3-dioxolan-2-one (Table 2, entry 1).

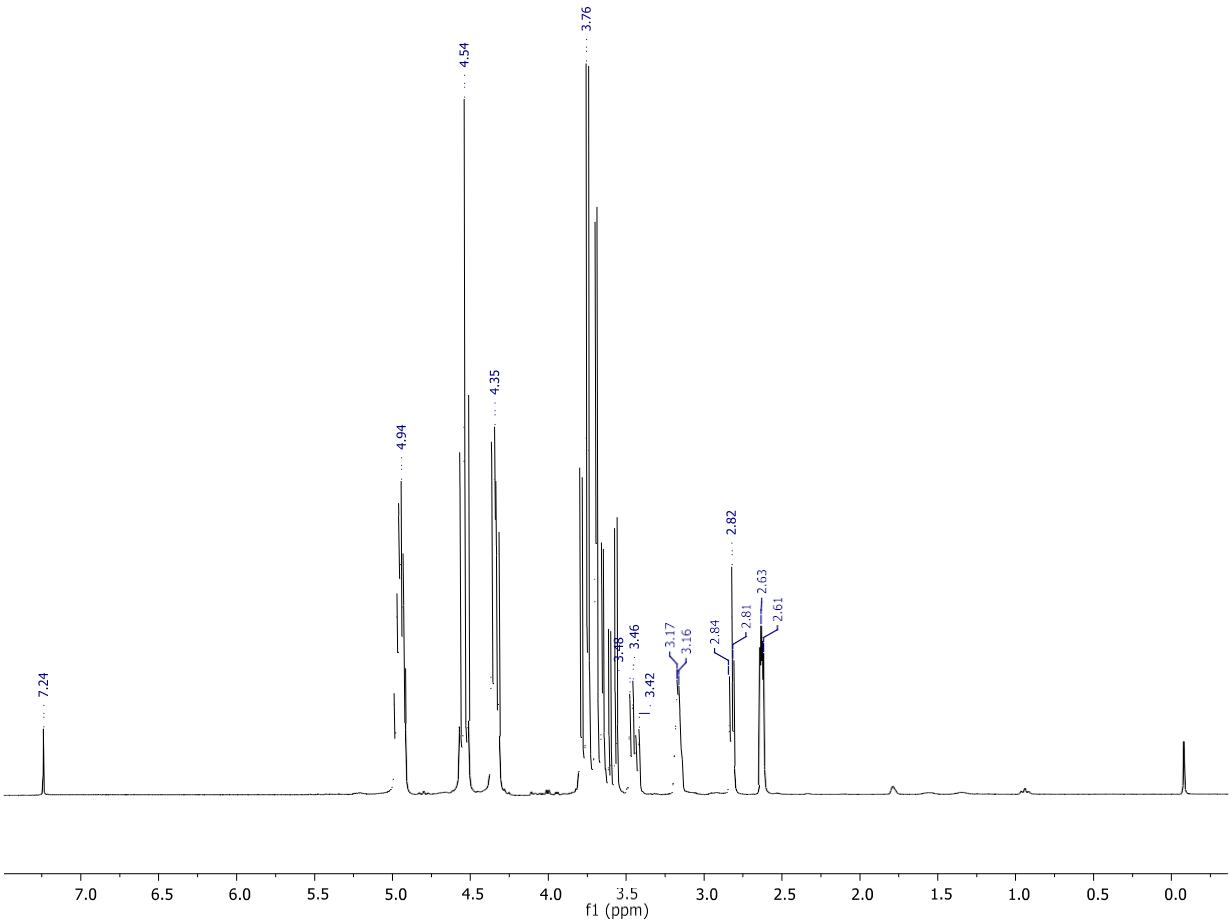

Figure S27. ^{1}H NMR spectrum (300 MHz, 298 K, $CDCl_3$) of 4-chloromethyl-1,3-dioxolan-2-one (Table 2, entry 2).

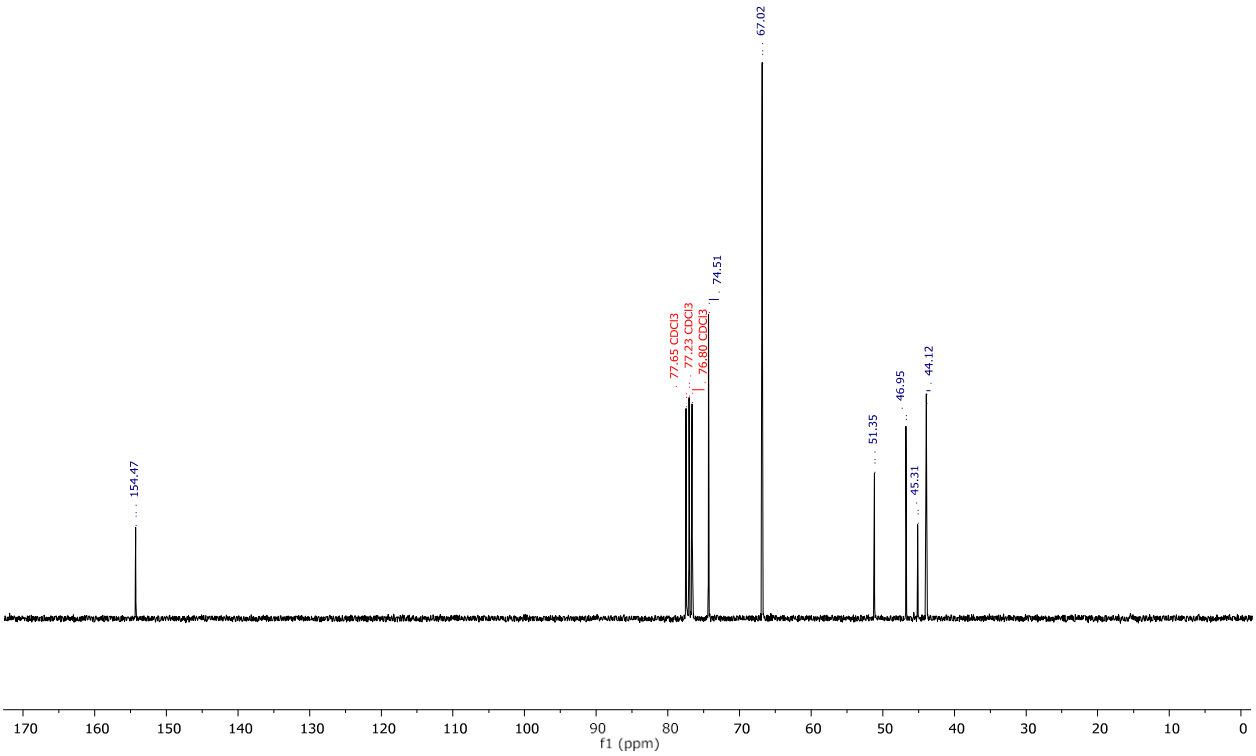

Figure S28. ^{13}C NMR spectrum (300 MHz, 298 K, $CDCl_3$) of 4-chloromethyl-1,3-dioxolan-2-one (Table 2, entry 2).

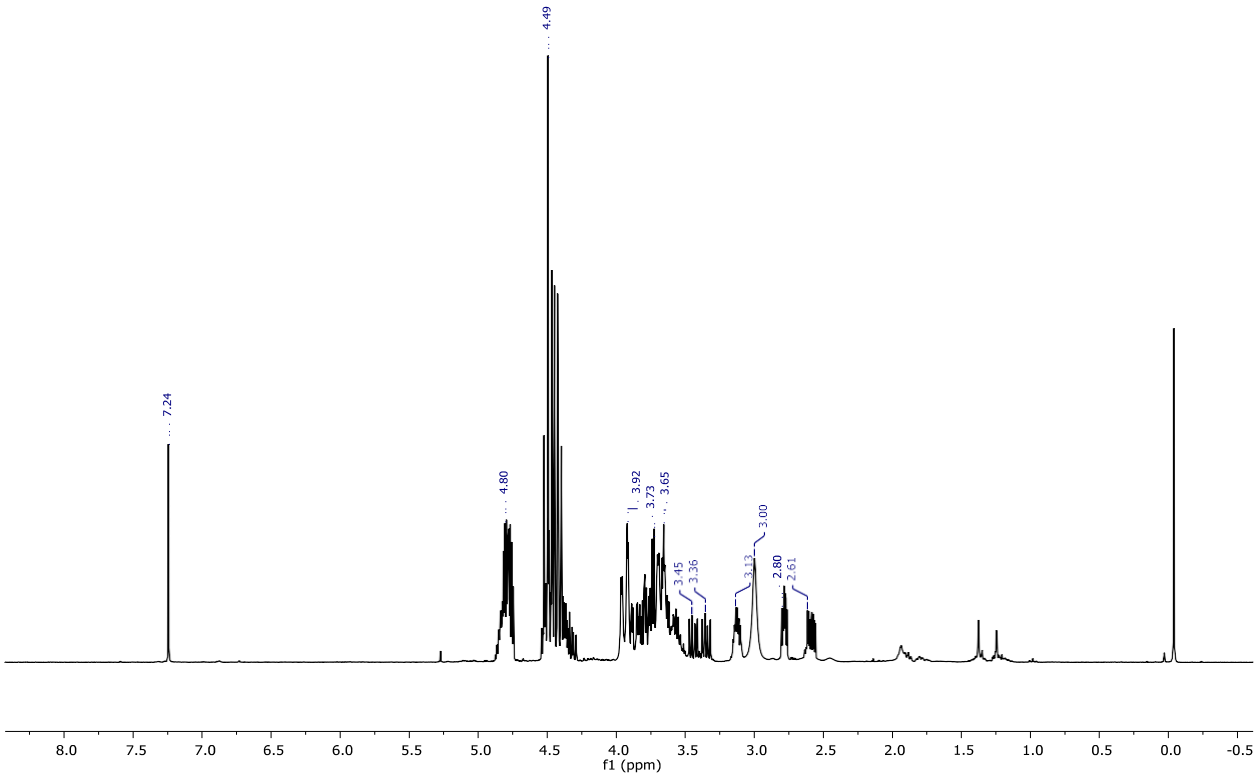

Figure S29. ^{1}H NMR spectrum (300 MHz, 298 K, $CDCl_3$) of 4-hydroxymethyl-1,3-dioxolan-2-one (Table 2, entry 3).

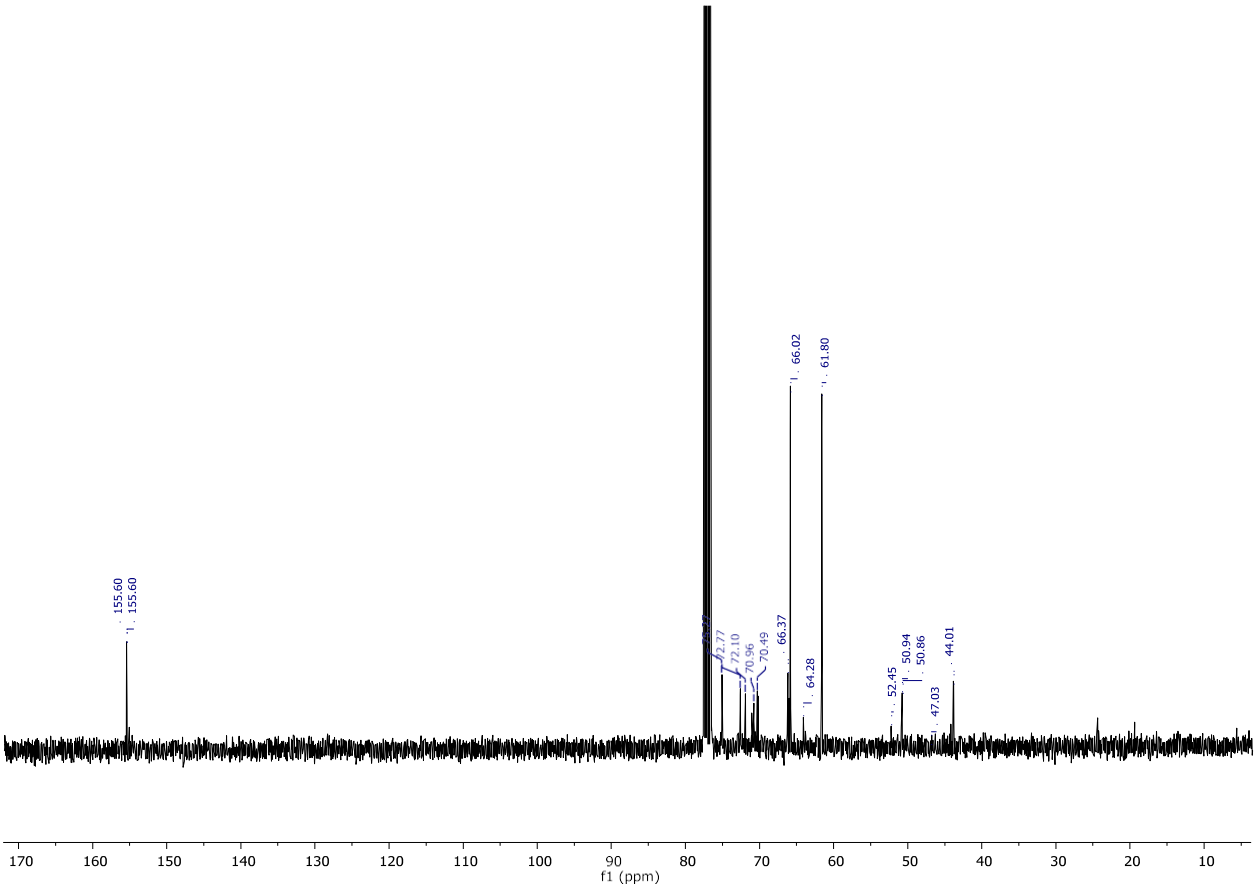

Figure S30. ^{13}C NMR spectrum (300 MHz, 298 K, $CDCl_3$) of 4-hydroxymethyl-1,3-dioxolan-2-one (Table 2, entry 3).

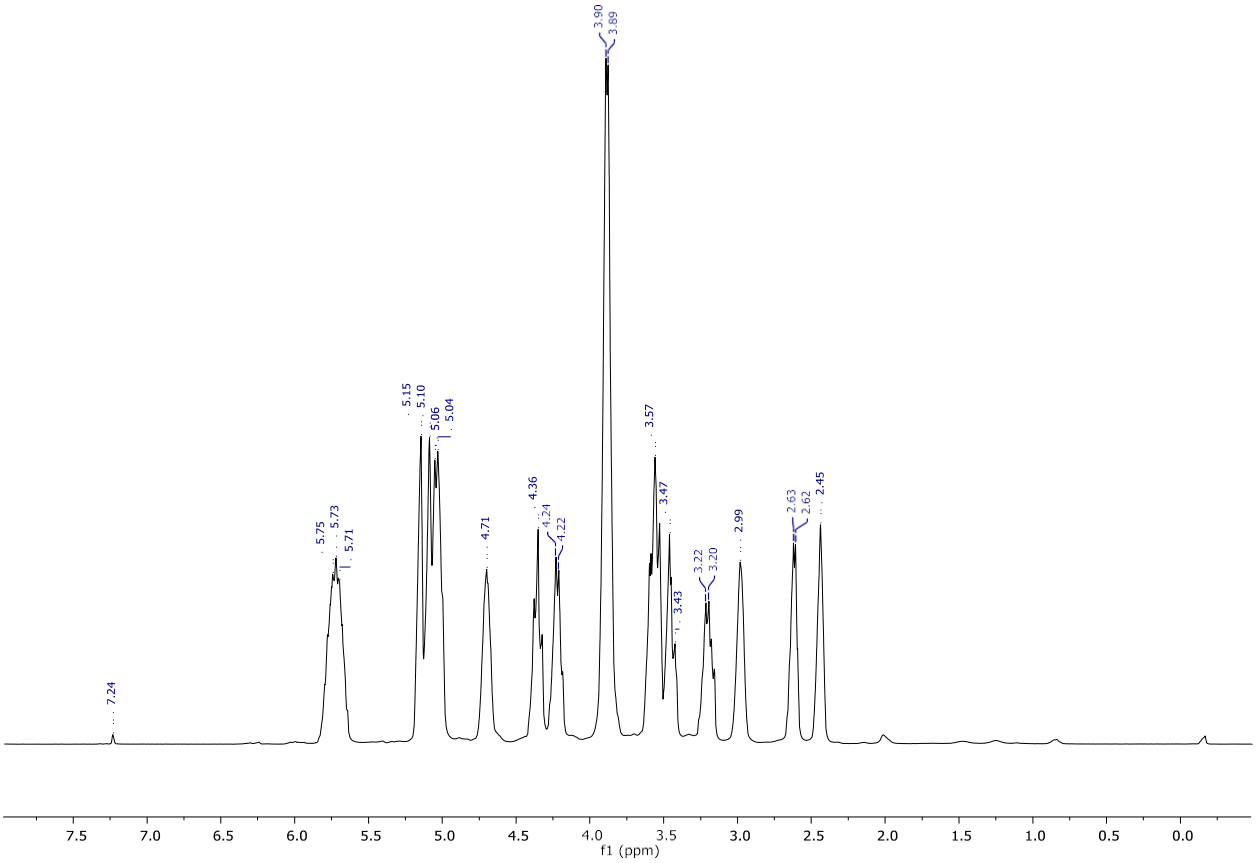

Figure S31. ^{1}H NMR spectrum (300 MHz, 298 K, $CDCl_3$) of 4-allyloxymethyl-1,3-dioxolan-2-one (Table 2, entry 4).

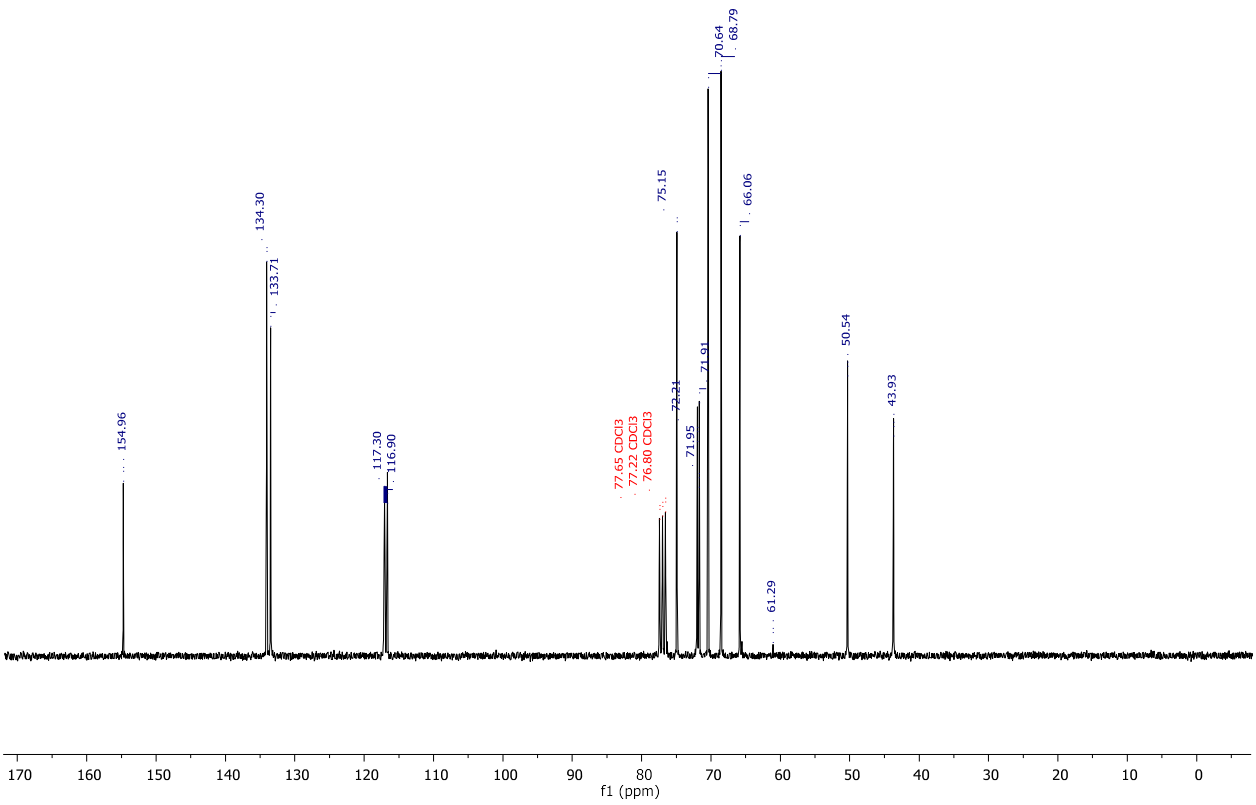

Figure S32. ^{13}C NMR spectrum (300 MHz, 298 K, $CDCl_3$) of 4-allyloxymethyl -1,3-dioxolan-2-one (Table 2, entry 4).

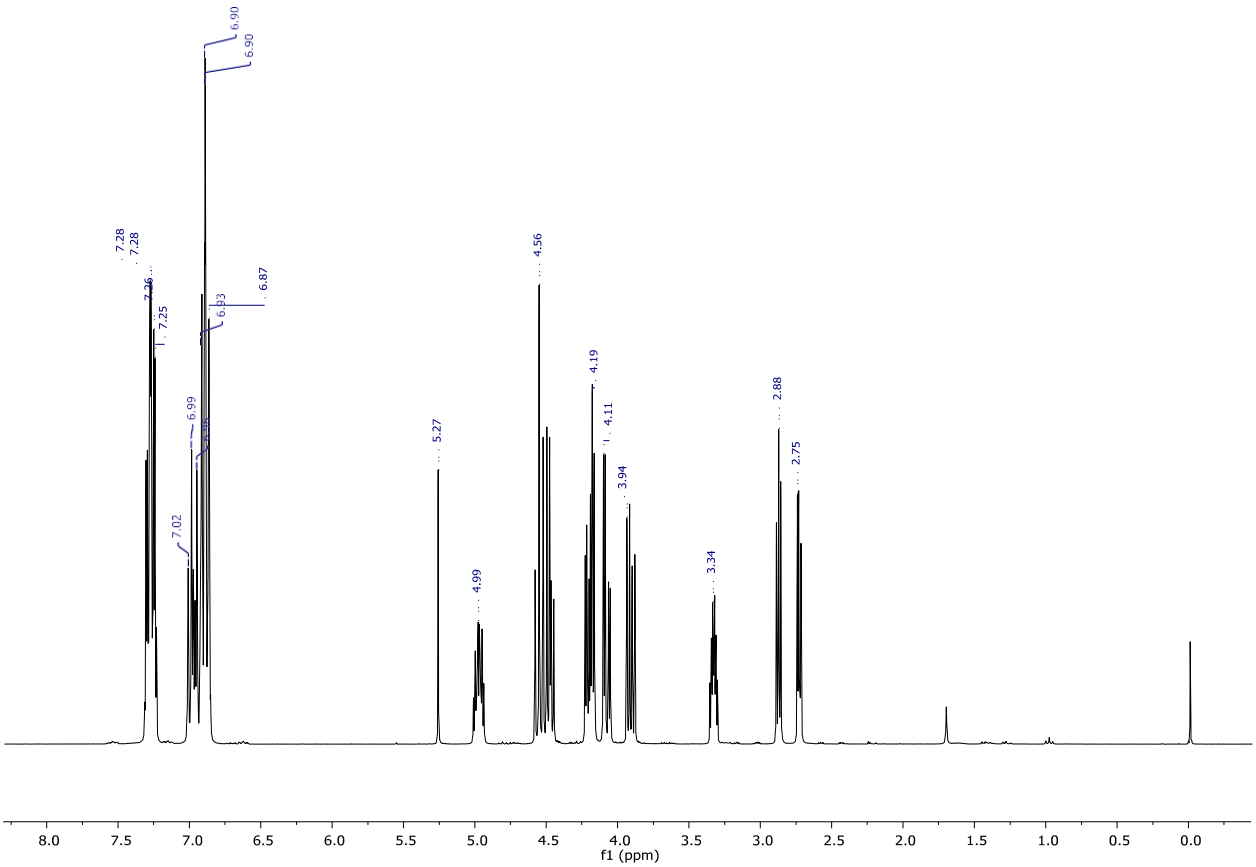

Figure S33. ^{1}H NMR spectrum (300 MHz, 298 K, $CDCl_3$) of 4-phenoxymethyl-1,3-dioxolan-2-one (Table 2, entry 5).

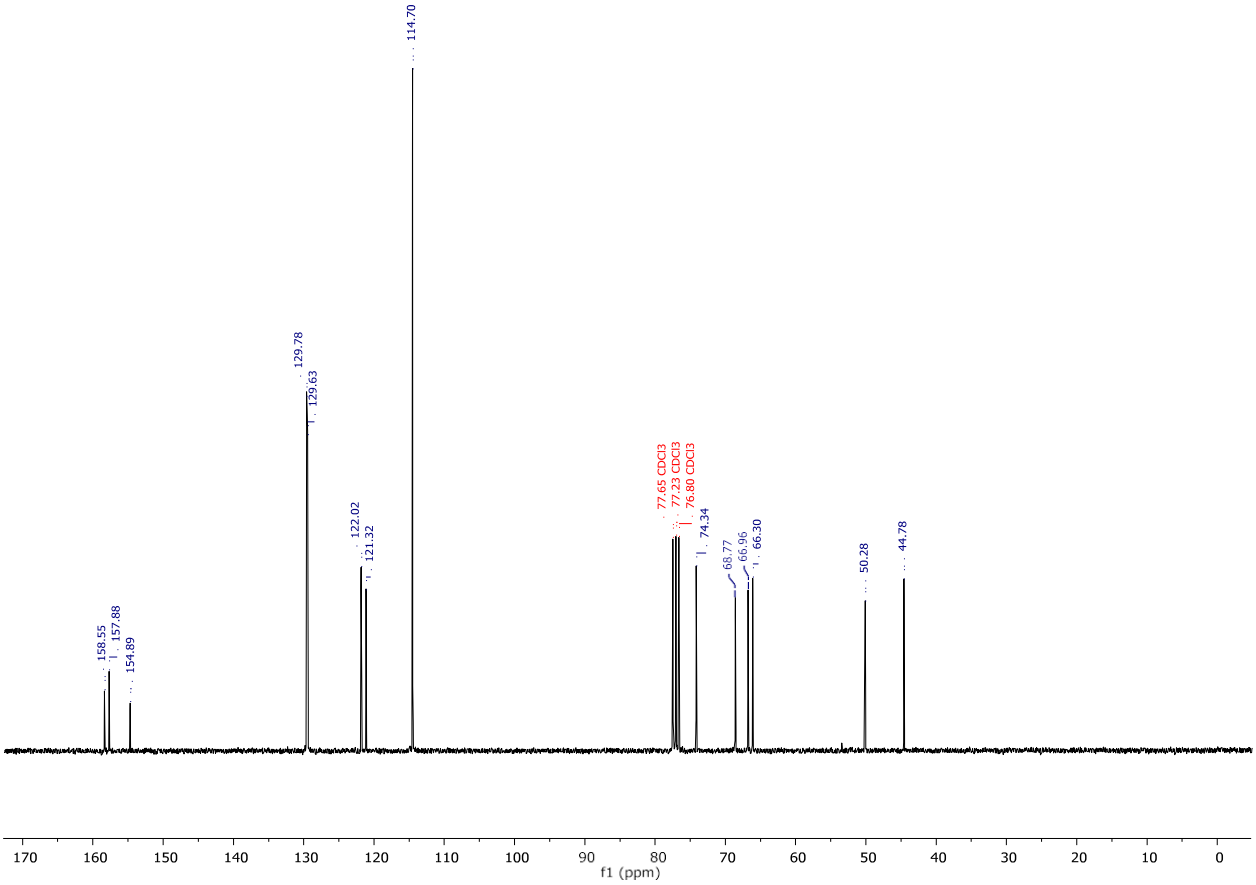

Figure S34. ^{13}C NMR spectrum (300 MHz, 298 K, $CDCl_3$) of 4-phenoxymethyl-1,3-dioxolan-2-one (Table 2, entry 5).

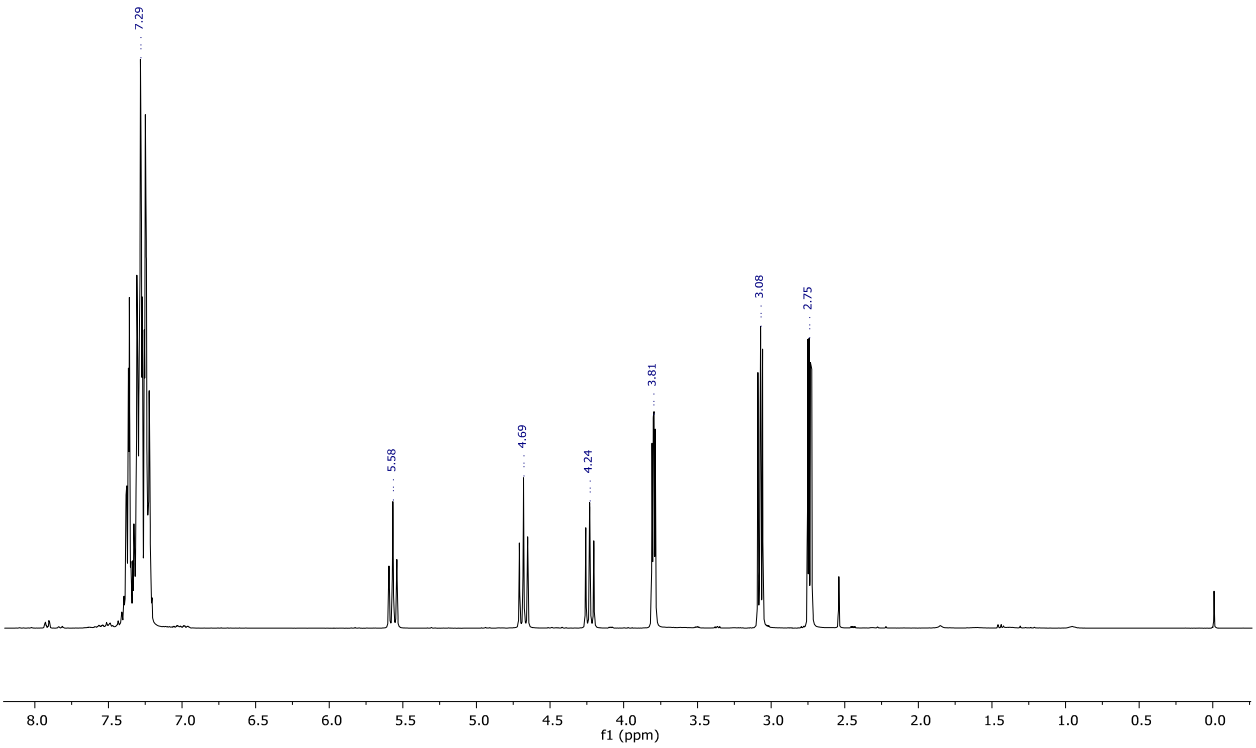

Figure S35. ^{1}H NMR spectrum (300 MHz, 298 K, $CDCl_3$) of 4-phenyl-1,3-dioxolan-2-one (Table 2, entry 6).

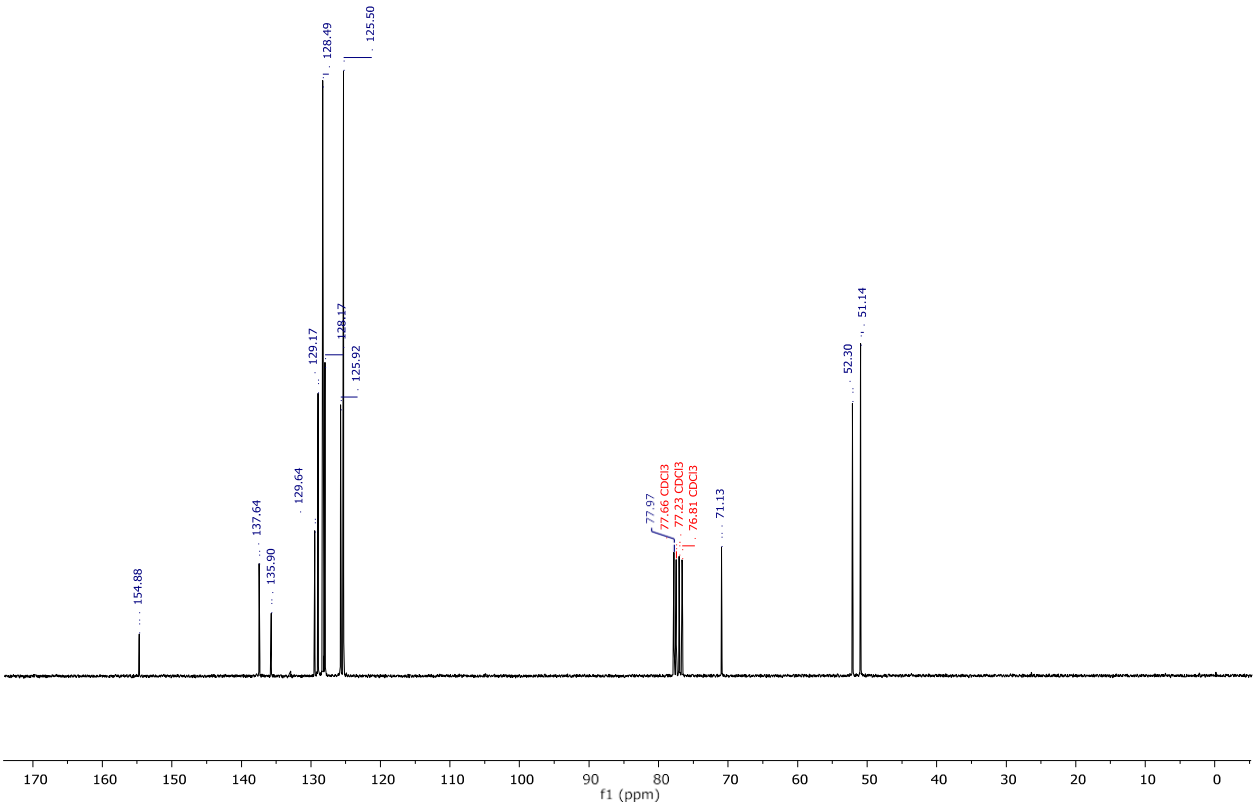

Figure S36. ^{13}C NMR spectrum (300 MHz, 298 K, $CDCl_3$) of 4-phenyl-1,3-dioxolan-2-one (Table 2, entry 6).

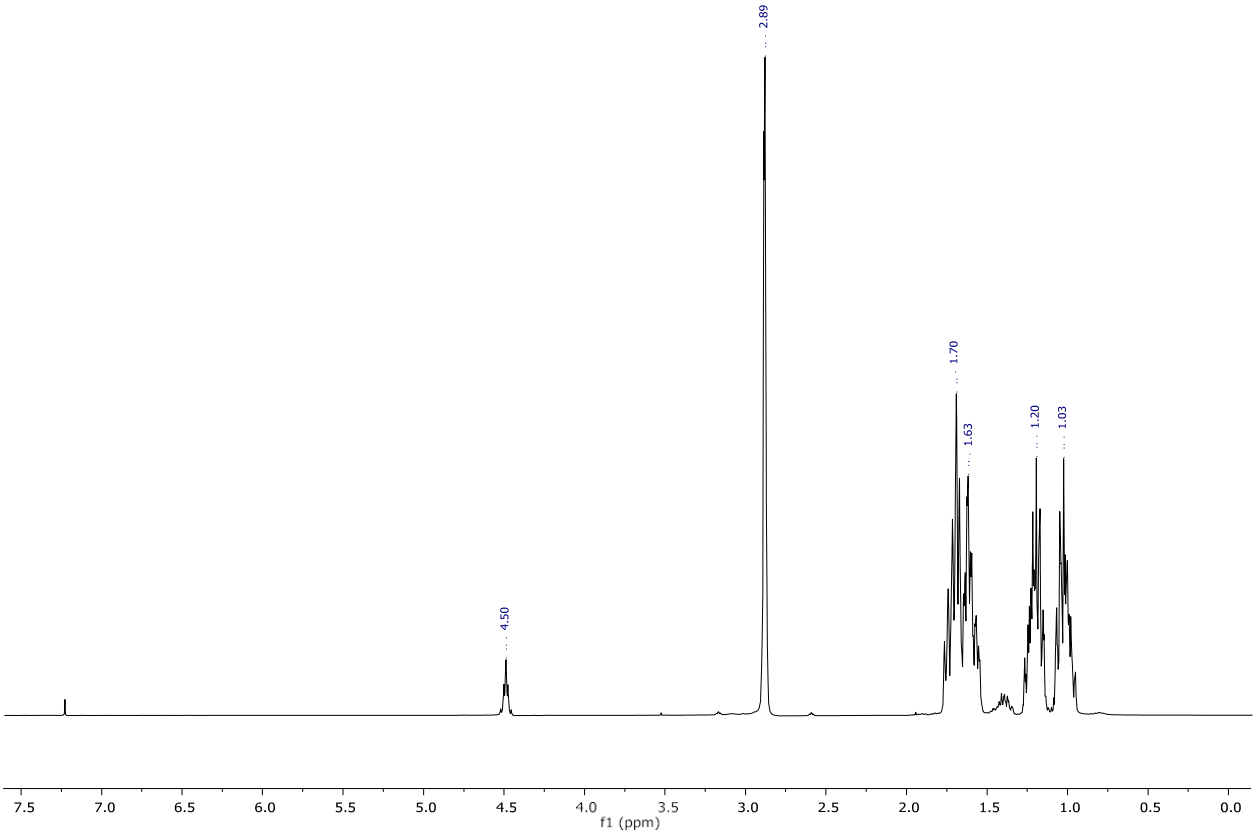

Figure S37. ^{1}H NMR spectrum (300 MHz, 298 K, $CDCl_3$) of cis-1,2-cyclohexene carbonate (Table 2, entry 7).

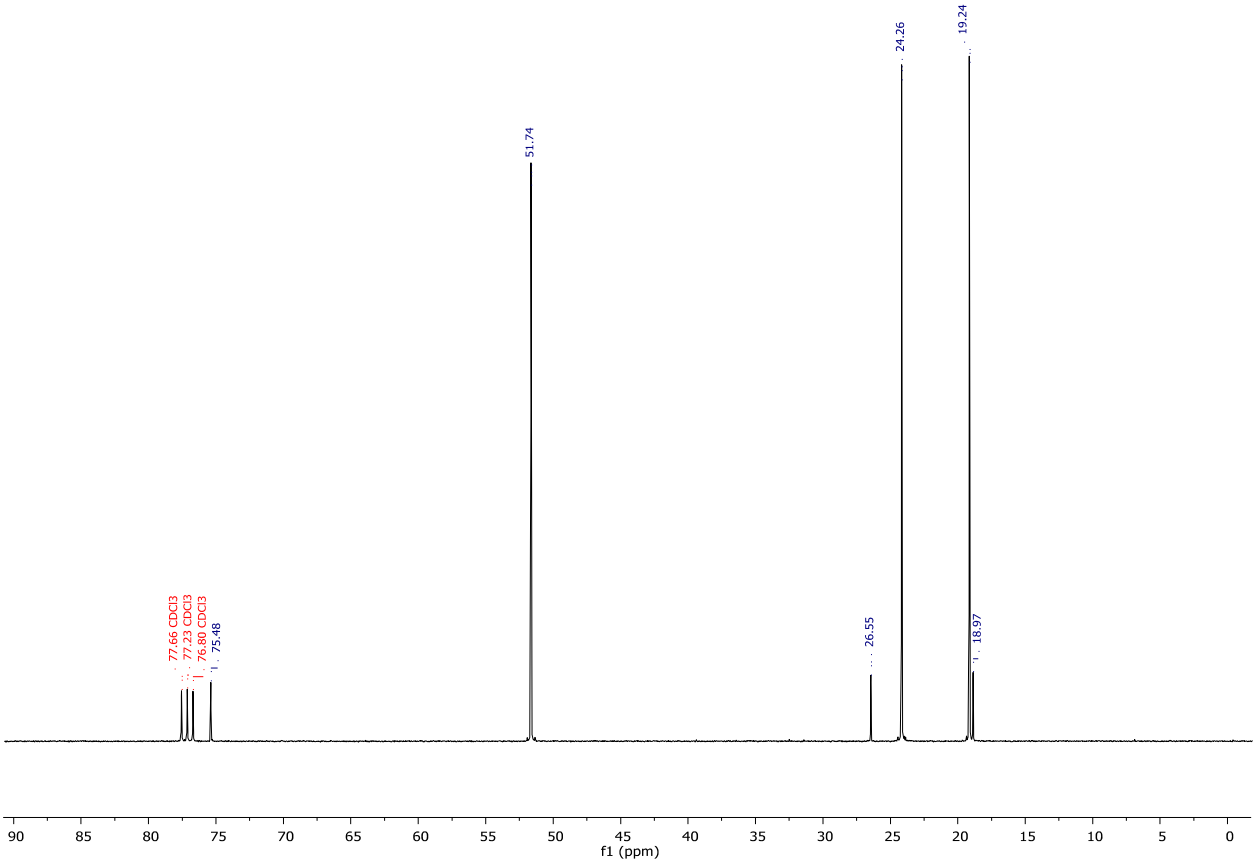

Figure S38. ^{13}C NMR spectrum (300 MHz, 298 K, $CDCl_3$) of cis-1,2-cyclohexene carbonate (Table 2, entry 7).